Biomaterials 35 (2014) 3975–3985

Contents lists available at ScienceDirect

Biomaterials

journal homepage: www.elsevier.com/locate/biomaterials

Spatial patterning of BMP-2 and BMP-7 on biopolymeric films and the guidance of muscle cell fate

Jorge Almodóvar [a,b,1], Raphaël Guillot [a,b], Claire Monge [a,b], Julien Vollaire [c], Šeila Selimović [d,e], Jean-Luc Coll [c], Ali Khademhosseini [d,e,f], Catherine Picart [a,b,*]

[a] CNRS UMR 5628 (LMGP), MINATEC, 3 parvis Louis Néel, 38016 Grenoble, France
[b] Université de Grenoble Alpes, Grenoble Institute of Technology, 3 parvis Louis Néel, 38016 Grenoble, France
[c] Institute Albert Bonniot, Grenoble, France
[d] Center for Biomedical Engineering, Department of Medicine, Brigham and Women's Hospital, Harvard Medical School, Cambridge, MA 02139, USA
[e] Harvard-MIT Division of Health Sciences and Technology, Massachusetts Institute of Technology, Cambridge, MA 02139, USA
[f] Wyss Institute for Biologically Inspired Engineering, Harvard University, Boston, MA 02115, USA

ARTICLE INFO

Article history:
Received 1 November 2013
Accepted 7 January 2014
Available online 30 January 2014

Keywords:
Bone morphogenetic proteins
Osteoinduction
Myogenesis
Layer-by-layer
Gradient
Microfluidic

ABSTRACT

In the cellular microenvironment, growth factor gradients are crucial in dictating cell fate. Towards developing materials that capture the native microenvironment we engineered biomimetic films that present gradients of matrix-bound bone morphogenetic proteins (BMP-2 and BMP-7). To this end layer-by-layer films composed of poly(L-lysine) and hyaluronan were combined in a simple microfluidic device enabling spatially controlled growth factor diffusion along the film. Linear long-range gradients of both BMPs induced the trans-differentiation of C2C12 myoblasts towards the osteogenic lineage in a dose dependent manner with a different signature for each BMP. The osteogenic marker alkaline phosphatase (ALP) increased in a linear manner for BMP-7 and non-linearly for BMP-2. Moreover, an increased expression of the myogenic marker troponin T was observed with decreasing matrix-bound BMP concentration, providing a substrate that it is both osteo- and myo-inductive. Lastly, dual parallel matrix-bound gradients of BMP-2 and -7 revealed a complete saturation of the ALP signal. This suggested an additive or synergistic effect of the two BMPs. This simple technology allows for determining quickly and efficiently the optimal concentration of matrix-bound growth factors, as well as for investigating the presentation of multiple growth factors in their solid-phase and in a spatially controlled manner.

1. Introduction

Growth factors are a powerful class of cell signaling molecules known to control multiple cellular events such as proliferation, migration and differentiation. Growth factors are secreted by cells and are subsequently trapped by proteoglycans in the native extracellular matrix (ECM), establishing gradients of signaling molecules [1]. The presentation of growth factors to cells—either soluble or in their solid-phase (also called "matrix-bound")—is crucial in dictating cellular fate [2]. The ECM is known to sequester growth factors and to present them to cells in a matrix-bound manner [1], mainly via natural affinity with matrix components such as glycosaminoglycans [3], proteins [4,5] and hydroxyapatite [6]. This natural affinity originates from a combination of interactions, including electrostatic, hydrophobic, and hydrogen bonds; however, the precise mechanisms are not yet understood. Using engineering methods, biomaterial scientists have thus made efforts to recreate these interactions in order to deliver growth factors locally to cells [7]. The strategies for presenting growth factors could be divided in two main categories: covalent binding and non-covalent binding (i.e. "matrix-bound") [8,9] to the biomaterial components. The former requires the elaboration of a synthetic route that does not alter the growth factor bioactivity, i.e. its active site should be available and in the appropriate conformation to allow molecular recognition by the cellular receptors, while the latter is a milder process but may lead to progressive release of the growth factor in contact with the cells. ECM components are thus particularly interesting for this second strategy in view of their natural biochemical and hydration properties. Biomaterials and coatings made of fibrin [10,11], collagen [12], and glycosaminoglycans (heparin [13], hyaluronan [14], etc.) have all been successfully developed for matrix-bound presentation of

* Corresponding author. Université de Grenoble Alpes, Grenoble Institute of Technology, 3 parvis Louis Néel, 38016 Grenoble, France.
E-mail address: catherine.picart@grenoble-inp.fr (C. Picart).
[1] Current address: Department of Chemical Engineering, University of Puerto Rico-Mayagüez, Mayagüez, PR 00681, USA.

0142-9612/$ – see front matter © 2014 Elsevier Ltd. All rights reserved.
http://dx.doi.org/10.1016/j.biomaterials.2014.01.012

several different types of growth factors, including epidermal growth factor (EGF) [9], basic fibroblast growth factor (FGF-2) [15], vascular endothelial growth factor (VEGF) [16] and bone morphogenetic protein 2 (BMP-2) [17]. Recently, thin coatings made of polypeptides and polysaccharides by the layer-by-layer (LbL) assembly technique [18] have also been shown to trap growth factors and to preserve their bioactivity [19,20]. The growth factors can be either incorporated into the LbL architecture [21] or adsorbed on top of it [22,23]. Successful examples include FGF-2 [24,13], brain derived neurotrophic factor (BDNF) [22] and BMP-2 [25].

Presenting growth factors in a spatially controlled manner is an additional step toward recreating the natural cellular microenvironment in order to combine both biochemical and topographical properties. Gradients of growth factors are naturally created during morphogenesis, where tissue patterns are guided by the presence of these signaling molecules [26]. Thus, researchers have proposed several approaches to create gradients of either soluble or covalently bound growth factors. Microfluidic devices are particularly advantageous for generating soluble gradients [27–30]. Covalent immobilization of growth factors in a gradient form could also be performed by several methods using chemical or photoactivated coupling strategies [9]. Several immobilized growth factors—including insulin-like growth factor-1 [31], EGF [31], and VEGF [16]—have been shown to increase cell migration. However, techniques for generating matrix-bound growth factor gradients (i.e. without covalent coupling) are still scarce. An inkjet printing technique was developed by Campbell and coworkers to form deposits of growth factors [10] such as FGF-2 and BMP-2 [32,10]. The amount of growth factor can be varied by overprinting it, which allows the formation of non-continuous growth factor gradients [33].

The bone morphogenetic proteins are an interesting class of growth factors playing a role in numerous physiological processes [34]. BMP-2 and BMP-7 are two members known for their osteoinductive properties [35], which have been approved for clinical use in specific applications [36]. Collagen sponge and paste are the only authorized matrices for BMP delivery, although collagen is known to have a very poor retention of BMP-2 [37]. Therefore, important efforts are currently devoted to engineering new materials for BMP delivery [38]. Interestingly, matrix-bound presentation has been shown to promote ossification at dosages lower than those used in soluble delivery [39–41]. Recently, Guldberg and coworkers demonstrated that higher doses and slower release of BMP-2 promoted increased bone formation, supporting the idea that a matrix-bound delivery is desirable [39]. Moreover, the spatial presentation of BMP is crucial to precisely control the location of the bone generated [40]. During morphogenesis, long-range gradients of BMPs are formed [42,43]. Recent studies investigated the potential of a sequential delivery of both BMP-2 and BMP-7 [44,45]. However, no study to date has aimed to present these two BMPs in a spatially controlled manner.

LbL films made of poly(L-lysine) (PLL) and hyaluronan (HA) are already known to retain a high amount of BMP-2 [14] which makes them attractive to present the growth factor to cells in a matrix-bound manner, LbL films made of poly(L-lysine) (PLL) and hyaluronan (HA) are already known to retain a high amount of BMP-2 [14], which makes them attractive to present the growth factor to cells in a matrix-bound manner. Matrix-bound BMP-2 also revealed a role of BMP-2 in cell adhesion and migration [25]. Recently, we used a simple microfluidic device [46] to create gradients of molecules (e.g. crosslinker, peptide) on these films [47]. Cells were found to respond to gradients of stiffness and of adhesion peptide concentration [47].

Here, we investigate the possibility to generate linear gradients of matrix-bound BMPs to study the spatial differentiation of BMP-responsive skeletal myoblasts [48,49], depending on the type and the amount of BMP presented by the film. In addition to BMP-2, BMP-7 was selected for several reasons: i) it is the second clinically approved growth factor to be used in bone regeneration therapies, ii) it is known that C2C12 behave differently in the presence of BMP-7 as compared to BMP-2 [35], and iii) no previous study had investigated the matrix-bound presentation of BMP-7 to cells. Combining LbL with a simple microfluidic device to spatially control growth factor presentation provide numerous perspectives for the study of cellular events, including adhesion, spreading, migration, and differentiation on an ECM mimetic material. Moreover, this technology may be used to quickly test a large range of growth factor concentrations for optimization purposes.

2. Materials and methods

2.1. Materials

Hyaluronan (HA, 3.5×10^5 g mol^{-1}) was purchased from Lifecore Biomedical LLC (USA). Poly(ethylenimine) (PEI), poly(L-lysine) (PLL, 5.6×10^4 g mol^{-1}), 1-ethyl-3-(3-dimethylaminopropyl) carbodiimide (EDC), phalloidin-tetramethylrhodamine B isothiocyanate, sigmafast *p*-nitrophenyl phosphate tablets, mouse anti-Troponin T primary antibody, 5(6)-carboxytetramethylrhodamine *N*-succinimidyl ester (RHO), 5(6)-carboxyfluorescein *N*-hydroxysuccinimide ester (FL), and 4′,6-diamidino-2-phenylindole dihydrochloride (DAPI) and *N*-hydrosuccinimide (sulfo-NHS) were purchased from Sigma (France). Alexa Fluor 647-conjugated secondary antibody and Prolong antifade Gold reagent were purchased from Molecular Probes-Invitrogen (France). Fetal bovine serum (FBS) and horse serum (HS) were purchased from PAA Laboratories (Les Mureaux, France). Recombinant human bone morphogenetic protein 2 (BMP-2) was purchased from Medtronic (Minnesota, USA) and recombinant human bone morphogenetic protein 7 (BMP-7) was kindly donated by Olympus Biotech (Massachusetts, USA). All other cell culture reagents were purchased from Gibco (Invitrogen, Cergy-Pontoise, France). All other salts, buffers, and solvents were purchased from Sigma and used as received. Ultrapure water with a resistivity of 18.2 MΩ was used for making all aqueous solutions (Milli-Q-plus system, Millipore, Molsheim, France).

2.2. Fluorescently-labeled BMPs

Rhodamine-labeled BMP-2 (BMP-2^{RHO}), and fluorescein-labeled BMP-2 or -7 (BMP-2^{FL}, and BMP-7^{FL}) were prepared by reacting the dye with the proteins (20 mol DYE:1 mol BMP) for 2 h at pH 7 in a sodium bicarbonate buffer (50 mM), and purifying using a Sephadex G25 column. A NanoDrop 2000 (Thermo Scientific) spectrophotometer was used to calculate the degree of labeling and protein concentrations. Degrees of labeling of 34%, 38%, and 41% were obtained for BMP-2^{RHO}, BMP-2^{FL}, and BMP-7^{FL} respectively.

2.3. LbL film buildup and BMPs loading

PEI (2.5 mg/mL), HA (1 mg/mL), and PLL (0.5 mg/mL) were dissolved in a filtered HEPES-NaCl buffer solution (20 mM HEPES, pH 7.4, 0.15 M NaCl). Substrates for LbL deposition were cleaned in a 0.5% Hellmanex (Hellma, Müllheim, Germany) solution and modified with an anchoring PEI layer. LbL films of 12 layer pairs built on glass substrates were prepared using an automated dipping machine (Dipping Robot DR3, Kirstein GmbH, Germany) as previously described on coverslips (dia. 14 mm) for experiments on homogeneous films or slides (25 mm × 75 mm × 1 mm, Menzel-Gläser, Germany) for experiments on gradients [50]. Films were crosslinked overnight with EDC at 10 mg/mL and sulfo-NHS at 11 mg/mL both dissolved in NaCl (0.15 M, pH 5.5) followed by extensive rinsing with HEPES-NaCl buffer solution. BMPs, dissolved in 1 mM HCl, were incorporated homogeneously into the films by incubation at 37 °C, followed by rinsing with HEPES-NaCl. For quantification of BMP-2 and -7 adsorbed amounts the films were built in 96-well plates (Greiner Bio-One, Germany). The adsorbed amount was obtained from the fluorescence remaining in the wells after thorough rinsing over 2 h using a TECAN Infinite 1000 microplate reader (Tecan, Lyon, France). This value was used as the amount incorporated in the films [14].

2.4. Generation of BMP-2 and -7 gradients on LbL films

Gradients of BMP-2 and -7 were generated on LbL films as previously described [47] and showed on Scheme 1. Briefly, a LbL-coated glass slide was first rinsed with water before being dried and placed in contact with the microfluidic device. The channels of the microfluidic device were filled with 1 mM HCl solution, and a concentrated drop (5 or 10 μL) of BMP-2$^{RHO\ or\ FL}$ or -7^{FL} was placed in the inlet, while a large drop (200 μL) of 1 mM HCl was left at the outlet. The difference in surface tension between the two drops generated a flow from inlet to outlet [46]. The sample was incubated for 40 min at room-temperature. During this incubation

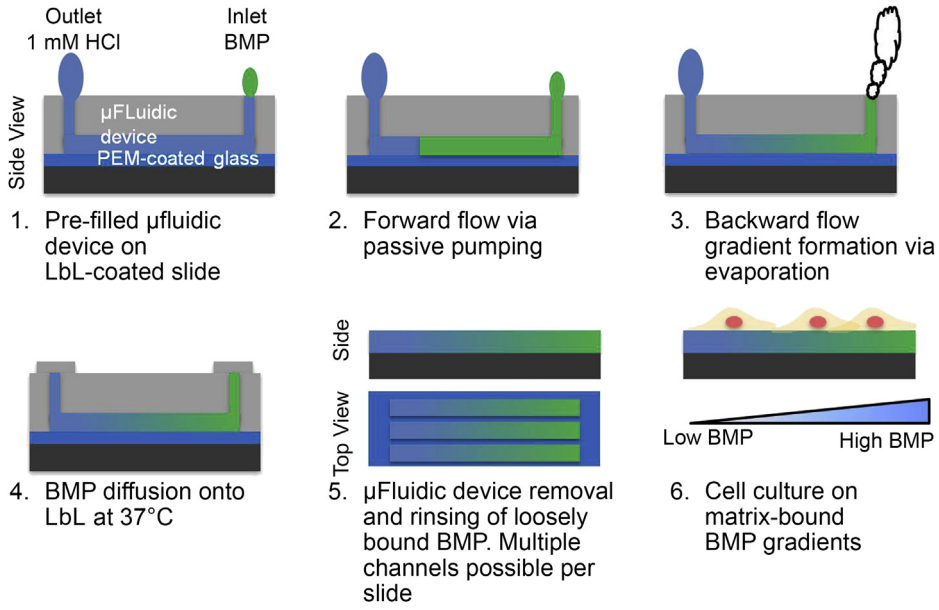

Scheme 1. Schematic representation of the different steps of matrix-bound gradient formation using microfluidics on a glass slide coated with (PLL/HA) films prepared via layer-by-layer assembly.

period, backward flow due to evaporation from the inlet occurred generating the BMPs gradient [46]. Afterwards, the inlet and outlet were sealed and the sample was incubated for an additional 90 min at 37 °C to allow the BMPs to diffuse in the films. The microfluidic device was then removed and the glass slide was extensively rinsed with HEPES-NaCl and stored until further use.

The matrix-bound BMPs gradients were visualized using a Zeiss LSM 700 microscope (Zeiss, Le Peck, France). Images were obtained every 1.28 mm throughout the length of the sample using an automated stage. Quantification of the fluorescence profiles were performed using ImageJ 1.46c (NIH, USA). Calibration curves of the different BMPs were obtained by loading FL labeled BMPs at known concentration on LbL films constructed in 96-well plates, calculating the amount of fluorescently-labeled BMPs retained after rinsing (using fluorescence measurements) and correlating those amounts to the fluorescent intensities obtained by fluorescence microscopy (see Fig. S1).

2.5. Bioactivity of matrix-bound BMP-2 and -7 on homogenous films

C2C12 myoblasts were used as a model cell type for investigating the bioactivity of matrix-bound BMP-2 and -7. All samples for cell culture were sterilized under UV light for 15 min and placed in wells of a Nuclon Δ-treated 24-well plate (Nunc ALS, Roskilde, Denmark). C2C12 cells (from ATCC, <20 passages) were cultured in a 1:1 Dulbecco's modified Eagle's medium (DMEM)/Ham's F12 medium supplemented with 10% FBS, containing 10 U/mL penicillin G and 10 μg/mL streptomycin growth media (GM). C2C12 cells were seeded on LbL-coated coverslips with matrix-bound BMP-2 and/or −7 at 60,000 cells/cm^2. Alkaline phosphatase (ALP) expression was quantified after 3 days of culture in GM as follows: the culture medium was removed and the cells were lysed by sonication over 5 s in 500 μL of 0.1% Triton-X100 in phosphate buffered saline (PBS). 180 μL of a buffer containing 0.1 M 2-amino-2-methyl-L-propanol (Sigma, St Quentin-Fallavier, France), 1 mM $MgCl_2$, and 9 mM *p*-nitrophenyl phosphate (Euromedex, Mundolsheim, France) adjusted to pH 10 was added to 20 μL of lysate. The enzymatic reaction was monitored in a 96-well plate by measuring the absorbance at 405 nm using the TECAN Infinite 1000 over 10 min. The total protein content of each sample was determined by using a bicinchoninic acid-based protein assay kit (Interchim, Montluçon, France). The ALP specific activity was expressed as μmoles of *p*-nitrophenol produced per min per mg of protein (pnp/min/mg), and then converted to relative expression by setting the highest ALP value obtained as 100%.

2.6. Bioactivity of gradients of matrix-bound BMP-2 and -7

Cellular response to BMP gradients was performed using C2C12 cells. All samples for cell culture were sterilized under UV light for 15 min and placed in wells of a Nuclon Δ-treated 4-well plate (Nunc ALS, Roskilde, Denmark). For luminescence imaging, C2C12 were transfected with an expression construct (BRE-Luc) containing a BMP-responsive element fused with the firefly luciferase reporter gene [51]. They were seeded on matrix-bound BMP-2 gradients at 35,000 cells/cm^2, cultured for 28 h, and exposed to D-luciferin potassium salt (Promega, Lyon, France) in PBS (final concentration 150 μg/mL) for 5 min prior to imaging with a back-thinned CCD cooled camera (ORCAII-BT-512G, Hamamatsu Photonics, Massy, France). For differentiation assays, C2C12 myoblasts were seeded at 10^4 cells/cm^2 and cultured in GM for 3 days prior switching to differentiation media (1:1 DMEM/F12 medium supplemented with 2% HS, containing 10 U/mL penicillin G and 10 μg/mL streptomycin) for two more days of culture. Afterwards, cells were fixed in 3.7% formaldehyde in PBS for 20 min and permeabilized for 4 min in Tris buffered saline (TBS, 50 mM Tris−HCl, pH 7.4, 0.15 M Nacl) containing 0.2% Triton X-100. Sigmafast *p*-nitrophenyl phosphate tablets were dissolved in water and used as directed by the manufacturer to visualize ALP expression on the gradient. Color images were obtained along the length of the gradient using an Olympus CKX41 inverted microscope equipped with a DP20 digital camera. Using ImageJ, the RGB images were converted to CYMK and the intensities for the cyan and magenta channels were added to quantify the expression of ALP along the gradients. For troponin T staining, the gradients were blocked in TBS containing 0.1% bovine serum albumin for 1 h, and were then incubated with mouse anti-troponin T (1:100) in TBS with 0.2% gelatin for 30 min. Alexa Fluor-647 conjugated secondary antibody was then incubated for 30 min with rhodamine-phalloidin (1:800). The nuclei were stained with DAPI at (0.1 μg/mL) for 10 min at room temperature. The slides were mounted onto coverslips with antifade reagent (Prolong, Molecular Probes, Saint Aubin, France) and imaged, as mentioned above, using a Zeiss LSM 700 microscope. Troponin T positive cells per field of view were counted along the channel of the gradients.

3. Results

3.1. ALP expression of C2C12 in the presence of BMP-2 or -7 delivered in solution

C2C12 myoblasts are known to commit towards the osteogenic lineage in the presence of bone morphogenetic proteins (BMPs) [48,49]. To compare the behavior of the different BMPs, a dose response to BMP-2 and BMP-7 was performed by measuring the expression of alkaline phosphatase (ALP) of C2C12 myoblasts after 3 days of culture. Both BMP-2 and -7 are capable of inducing the ALP expression of C2C12 myoblasts, albeit their dose response is different (Fig. 1). BMP-2 induces quantifiable ALP expression at a concentration of 50 ng/mL reaching a saturation level at 400 ng/mL. However, higher concentrations of BMP-7 were required for comparable levels of ALP expression, with a minimum expression at 250 ng/mL and a saturation concentration at 4000 ng/mL. Dose response curves yields inflection points of 117 ng/mL and 858 ng/mL for BMP-2 and BMP-7 respectively. Based on these results a 7× larger BMP-7 dose is required compared to BMP-2 to induce the expression of ALP in myoblast cells after 3 days of culture.

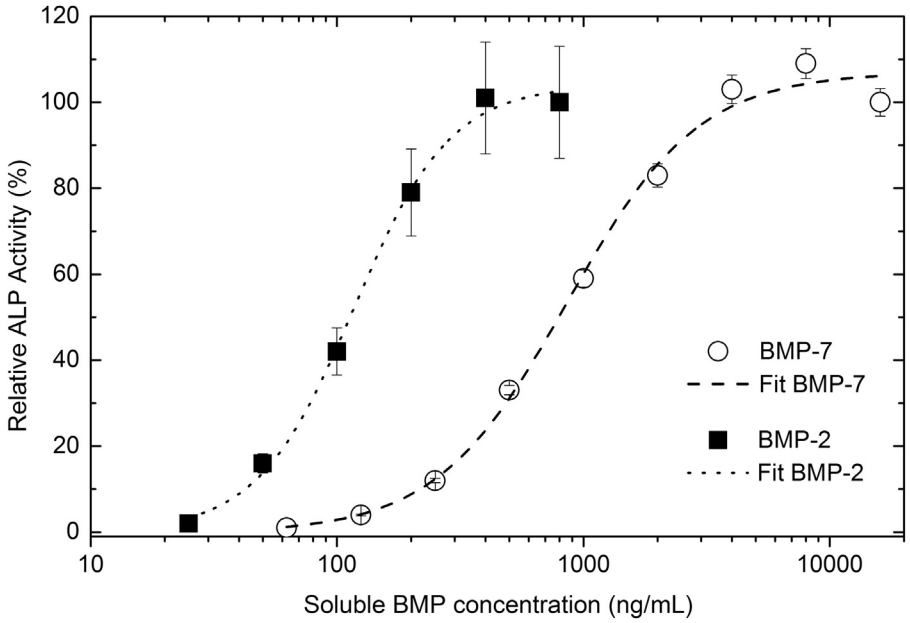

Fig. 1. ALP expression of C2C12 myoblasts in response to soluble BMP-2 and BMP-7 added at increasing concentrations. ALP was measured after 3 days of culture using a colorimetric assay. Dose response curves yield inflections points of 117 ng/mL and 858 ng/mL respectively for BMP-2 and BMP-7. Error bars indicate standard deviation of five samples.

3.2. Characterization of matrix-bound BMP-2 or -7 on homogeneous films

We have previously shown that crosslinked LbL films made of PLL and HA serve as a reservoir for BMP-2 and that BMP-2 is stable in the films after thorough rinsing and drying [14,52]. Moreover, these (PLL/HA) films can be used to coat osteogenic ceramic or titanium implants for the delivery of BMP-2, which promote higher bone formation than the implants alone or with BMP-2 delivered in solution [53,54]. In this work, (PLL/HA) films were investigated as a potential carrier of BMP-7. Cross-linked films of 12 layer pairs were loaded with BMP-7 with solutions of varying concentrations. Experiments with BMP-2 were done in parallel for comparison. Using fluorescently labeled BMPs the absorbed amounts of BMPs were monitored as a function of initial loading concentration (Fig. 2A). A maximum loading value of 1.8 ± 0.5 μg/cm^2 of BMP-7 was reached when the initial BMP-7 concentration was 100 μg/mL (Fig. 2A). For BMP-2 higher loading values could be obtained with higher initial loading concentrations such as 6.6 ± 0.4 μg/cm^2 for an initial concentration of 100 μg/mL (Fig. 2A). Both matrix-bound BMP-2 and -7 are capable of inducing ALP expression of C2C12 myoblasts after 3 days of culture in a dose dependent manner (Fig. 2B). The behavior of matrix-bound BMPs is similar to when delivered in solution in that BMP-2 induces ALP expression at lower concentrations compared to BMP-7. However, the profile curves are different between the two BMPs. BMP-2 exhibits a very steep slope before reaching a plateau value whereas BMP-7 exhibits a sigmoidal behavior. Also, matrix-bound BMP-2 induces a quicker ALP response reaching close to saturation levels (80% activity) at concentration of ~0.2 μg/cm^2, whilst higher concentrations of matrix-bound BMP-7 are needed to reach saturation level (~1.8 μg/cm^2).

3.3. Gradients of matrix-bound BMP-2 or -7

Gradients of matrix-bound BMPs on LbL films were generated by means of a microfluidic device (Scheme 1). Briefly, in a first step, (PLL/HA) films were constructed on glass slides via the LbL method, rinsed, and air dried. A PDMS microfluidic device was placed in contact with the film. Then 1 mM HCl was introduced inside the microchannels leaving a large drop (~100 μL) in the outlet. A concentrated small drop (5 μL) of BMP was placed in contact with the inlet (Scheme 1, step 1). Due to surface tension difference a forward-flow occurs from inlet to outlet (Scheme 1, step 2), whilst a backward flow occurs due to evaporation (Scheme 1, step 3) [46]. After gradient formation in the microchannel, the sample is sealed and incubated at 37 °C to allow diffusion of BMP in the film (Scheme 1, step 4). Lastly, the microfluidic device was removed and the film was rinsed (Scheme 1, step 5) and sterilized prior to cell culture (Scheme 1, step 6). Considering the dose difference between BMP-2 and BMP-7 (Figs. 1 and 2), different initial loading concentrations were selected to generate the gradients (100 μg/mL for BMP-2 and 200 μg/mL for BMP-7). The matrix-bound BMPs gradients were visualized using fluorescently labeled BMP-7 (Fig. 3A in green) and BMP-2 (Fig. 3B in red). Fluorescent microscopy images revealed continuous and stable matrix-bound BMPs gradients over a distance of 25 mm. Using quantitative fluorescence microscopy and spectroscopy, quantification of the fluorescent profiles of the BMPs gradients was possible (SI Fig. 1). BMP-2 had a maximum loading surface concentration of ~2.0 μg/cm^2, while BMP-7 reached a maximum loading concentration of ~2.5 μg/cm^2. These long-range BMP gradients were linear over ~20 mm. Their slopes were respectively of 0.58 μg/cm^3 for BMP-2 and 1.24 μg/cm^3 for BMP-7. To further assess the bioactivity of the BMP gradient, we first observed the activation of the SMAD pathway using C2C12 myoblasts transfected with a luciferase reporter gene for the BMP-responsive element Id1 (when the SMAD pathway is activated) [51]. The activation of SMAD was observed to be dose dependent of matrix-bound BMP-2 (Fig. 4). The long-term bioactivity of the BMPs gradients was assessed by the trans-differentiation capacity of the skeletal myoblasts towards the osteogenic lineage. To this end, cells deposited on the BMP-2 or BMP-7 gradients were cultured in myogenic conditions, i.e. standard conditions that promote myoblast differentiation into myotubes in the absence of BMPs. This condition consists of 3 days in growth medium and 2 days in myoblast differentiation medium for a total of 5 days of culture. Figs. 5 and 6 show microscopic observations and quantification of

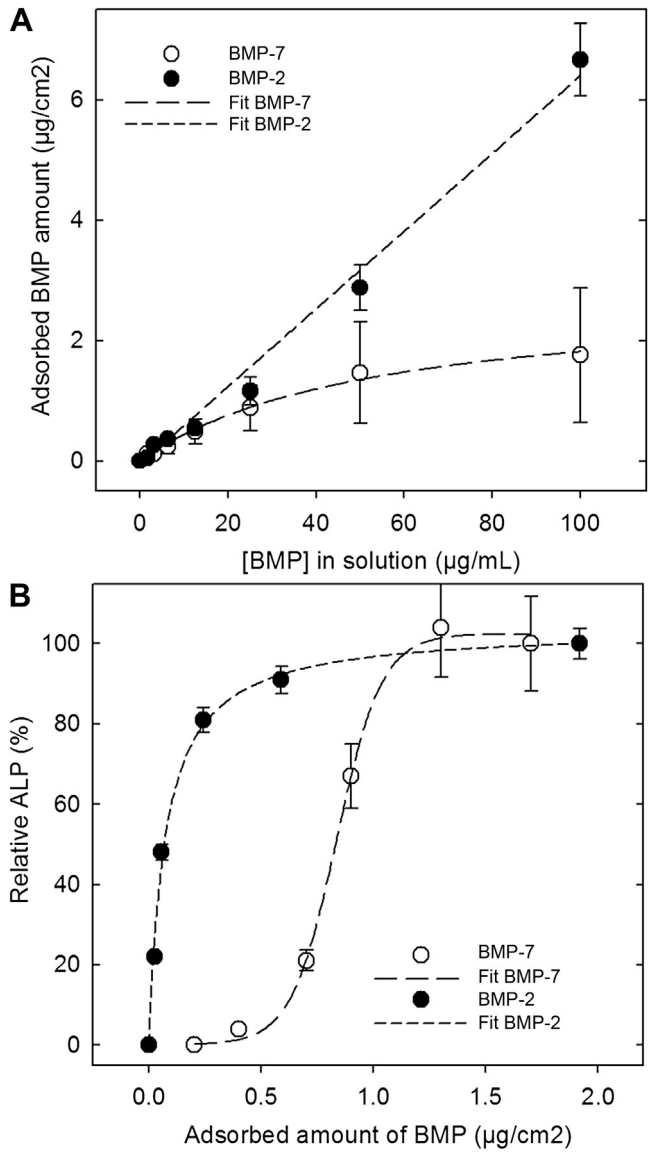

Fig. 2. (A) Adsorbed amounts of BMPs on (PLL/HA) films as a function of initial loading concentration of BMP-2 and BMP-7 in solution. BMP-7 data were fitted with a ligand binding curve (K_d = 56 µg/mL) whereas BMP-2 data were fitted with a linear regression (B) Relative ALP activity of C2C12 myoblasts on BMP-loaded (PLL/HA) films as a function of the adsorbed amount of BMP measured using a colorimetric assay. The highest BMP concentration for each condition was set at 100%. Error bars indicate standard error of three different experiments. BMP-7 data were fitted with a sigmoidal curve (inflection point at 0.8 µg/cm^2) whereas BMP-2 data were fitted with a ligand binding curve (K_d = 0.07 µg/cm^2).

the differentiation of myoblasts on the BMP-2 and BMP-7 gradients, where Troponin T positive cells (marker of differentiating myoblasts in myotubes) and ALP positive cells (marker of bone differentiation) were observed. Myoblasts responded to the BMP-2 gradients by expressing ALP along the length of the gradients (Fig. 5A). Of note, few myotubes were still visible at the lowest BMP concentration of the BMP-2 gradient.

Quantification of the ALP marker reveals a very low (close to zero) expression of ALP between 0.0 µg/cm^2 and 1.0 µg/cm^2 of matrix-bound BMP-2 followed by a sharp increase of expression (1.1 µg/cm^2 – 1.4 µg/cm^2), and a saturated expression after 1.4 µg/cm^2 to the matrix-bound BMP-2 gradient (Fig. 5B). The expression of troponin T positive cells decreased sharply between 0.0 µg/cm^2 – 1.0 µg/cm^2. In the region between 1.0 µg/cm^2 and 1.1 µg/cm^2, myoblast expressing both ALP and troponin T were observed (albeit no fusion was observed, Fig. 5A). In the regions of the gradient with no detectable BMP-2 myotube formation (fusion) was observed (SI Fig. 2). Of note, the matrix-bound BMP-2 gradient was retained even after the culture period as evidenced by the lack of ALP positive cells on regions outside the gradient, and by the retention of the fluorescent profile after 5 days of culture (SI Fig. 3). The length of the gradient could also be adjusted by changing the volume of the loading solution [46]. Increasing the loading volume of BMP-2 yielded longer bioactive matrix-bound BMP-2 gradients, with an ALP and troponin T expression profiles similar to the shorter gradients (SI Fig. 4). The behavior of myoblasts on the BMP-7 gradients was substantially different than that on the BMP-2 gradient (Fig. 6A). The expression of ALP continuously increases throughout the length of the gradient, while troponin T expression gradually decreases (Fig. 6B). ALP is expressed on areas outside of the gradients, although the gradient region is clearly visible (Fig. 6A). Longer regions of myoblasts expressing both osteo- and myogenic markers are observed in the BMP-7 gradients. Myotubes were also observed outside of the BMP-7 gradients (SI Fig. 2).

3.4. Dual matrix-bound BMP-2 and BMP-7 gradients on LbL films

To investigate a possible synergistic effect of BMP-2 and BMP-7 on cells, we first studied the ALP response on homogeneous films loaded with increasing amount of BMP-2 (loading concentrations of 3 and 6 µg/mL), for a fixed BMP-7 concentration (loading concentration 10 µg/mL) (Fig. 7A). As a control, BMP loading concentrations that are known to reach ALP saturation levels (50 µg/mL for BMP-7 and 25 µg/mL for BMP-2 respectively) were also investigated (Fig. 7A). Interestingly, the ALP signal in the presence of both BMP-2 and BMP-7 was close to the sum of the signals when BMP-2 and BMP-7 were delivered separately. The potential for matrix-bound BMP-7 to induce ALP expression is enhanced with small amounts of matrix-bound BMP-2. This suggests that BMP-2 and BMP-7 had an additive effect on C2C12 myoblasts.

Next, we generated dual gradients of both BMP-2 and BMP-7. These gradients could be in parallel (Fig. 7B) or opposite (Fig. 7C) depending on where the BMPs are introduced. Both solutions were placed in the inlet in the case of parallel gradients or opposite in the case of opposite gradients. Their quantification was possible by using two different fluorescent dyes in each BMP. Loading both BMPs in the same channel yields similar fluorescent profiles as loading them individually (Figs. 3 and 7B). The concentration of BMP-2 and BMP-7 increased with slopes of 0.8 µg/cm^3 and 1.0 µg/cm^3 for BMP-7. The presence of both BMPs did not impede the adsorption of one or the other.

ALP staining was used to test the bioactivity of the dual parallel gradient (Fig. 8). When delivered together, ALP expression was completely saturated and a high ALP expression was also observed on areas outside the gradients (Fig. 8A). This was not previously observed in the individual gradients. In addition, no obvious dose response was observed on the dual BMP gradient with respect to ALP expression and no troponin T positive cells were found. These data suggest an additive or synergistic effect between BMP-2 and BMP-7.

4. Discussion

C2C12 myoblasts are known to commit towards the osteogenic lineage in the presence of several bone morphogenetic proteins (BMPs) [48,49]. Our *in vitro* results using the ALP test showed that soluble BMP-2 is more potent than BMP-7 for inducing the transdifferentiation of C2C12 myoblasts. In addition, the dose response to BMP-2 and BMP-7 was significantly different as cells responded

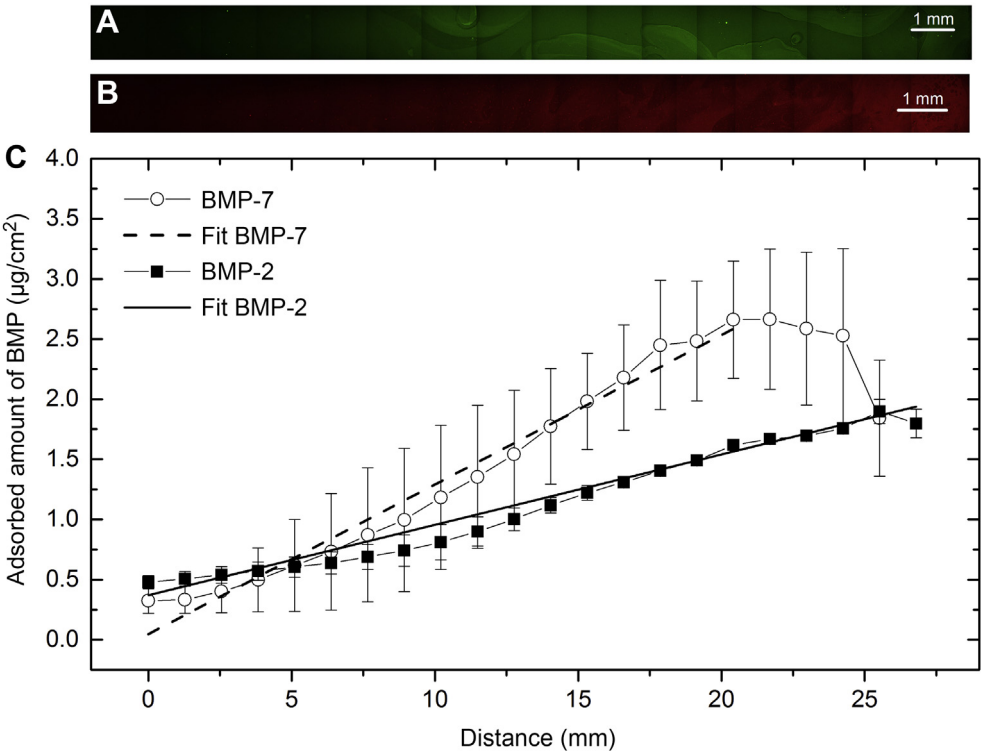

Fig. 3. Fluorescence images of matrix-bound gradients of fluorescein-labeled BMP-7 (A) and rhodamine-labeled BMP-2 (B) over one microchannel (scale bar: 1 mm). (C) Profiles of matrix-bound BMP gradients as a function of length of the channels. Adsorbed amounts were calculated from calibration curves obtained from a fluorescent plate reader and fluorescent microscopy (SI Fig. 1). Linear fits yields slopes of 0.58 μg/cm^3 and 1.24 μg/cm^3 for BMP-2 and BMP-7 respectively. Error bars indicate standard deviation between three different channels.

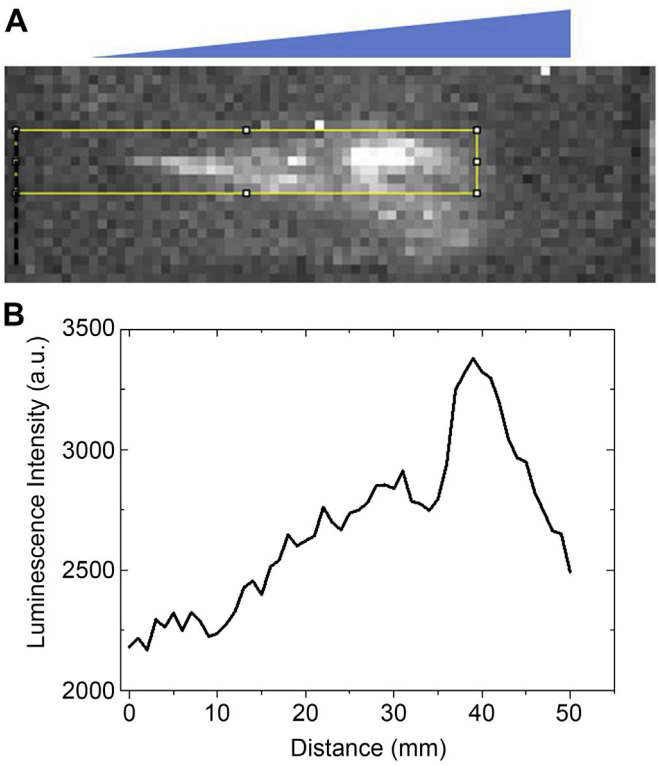

Fig. 4. (A) Luminescence imaging of C2C12 myoblasts transfected with a BMP-2 responsive element on a matrix-bound BMP-2 gradient, indicating dose–response activation of the SMAD pathway. Boxed region indicates approximate localization of the matrix-bound BMP-2 gradient. (B) Corresponding intensity profile as a function of the distance along the gradient.

in an "on/off" manner to BMP-2 but to a more gradual manner to BMP-7 (Fig. 1). In a previous study, He and coworkers [35] infected several mesenchymal progenitors (C3H10, C2C12 and TE-85 cells) with recombinant adenoviruses expressing fourteen human BMPs (BMP-2 to BMP-15). They found that BMP-2, 4, 6, 7 and 9 were all able to induce ALP activity in C2C12 cells and that osteoinduction potential was the highest for BMP-2 and BMP-9. In their study, it was impossible to investigate a dose response, as the cells secreted the BMPs. Barr et al. [55] also found a superior *in vitro* activity of BMP-2 as compared to BMP-7 but found *in* vivo that OP-1 (the kit containing BMP-7 for clinical applications) exhibited superior properties to Infuse (the kit containing BMP-2 for clinical applications). Thus, our *in vitro* results qualitatively agree with these previous studies regarding the differential BMP-7 versus BMP-2 response at specific time points.

We showed here that BMP-7 can be loaded in (PLL/HA) films and presented in a "matrix-bound" manner to cells. We have previously shown that (PLL/HA) films serve as reservoir of BMP-2 and that its bioactivity was retained [14,52]. The combination of LbL films with BMP-2 has also been investigated with other polyelectrolyte pairs [56,57,21]. However, the combination of BMP-7 with LbL films has barely been investigated. Tabrizian et al. used a liposome core coated with LbL films of chitosan and alginate for the controlled released of BMP-7 [58,59]. They demonstrated that the combination of LbL-coated particles with BMP-7 yielded higher osteogenic differentiation than all of the other conditions including the protein alone [58]. To our knowledge, the behavior of C2C12 on matrix-bound BMP-7 has not been previously investigated. We can tune the amount of BMP-7 loaded onto the films, which leads to a tunable expression of ALP expression of C2C12 (Fig. 2). This demonstrates the versatility of (PLL/HA) films to serve as growth factor reservoirs and to be used to present growth factors in a matrix-

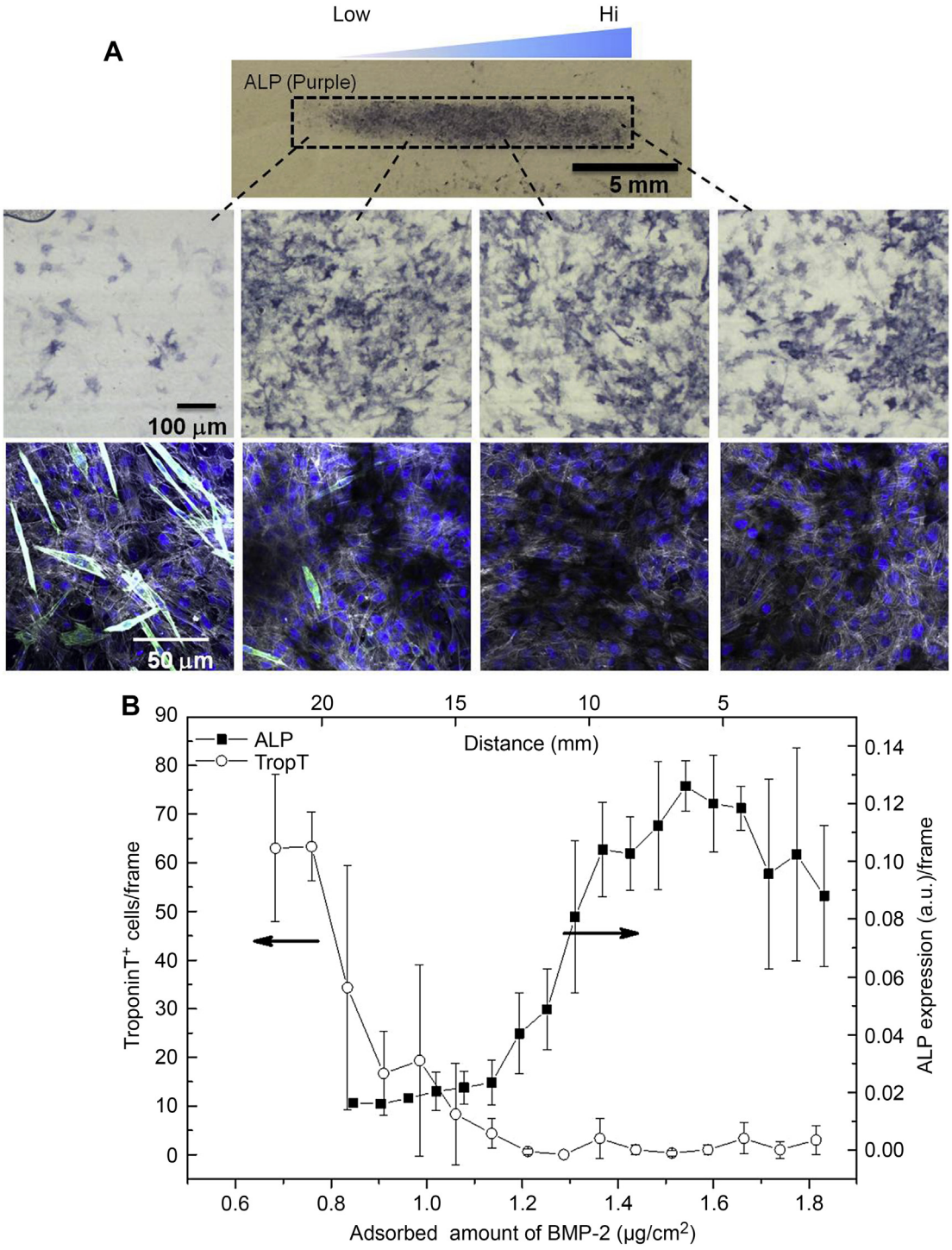

Fig. 5. Differentiation of C2C12 myoblasts on BMP-2 gradients. (A) Overview image and representative images of ALP staining confirm osteogenic differentiation, while immunofluorescent imaging reveals a decrease of troponin T positive cells (undergoing myogenic differentiation) with increasing BMP-2 concentration. Top images: ALP (purple); bottom images ALP (black), troponin T (green), actin (gray), nucleus (blue). (B) Quantification of ALP expression by measuring the intensities of the cyan and magenta channels in CMYK images, and amount of troponin T positive cells per field of view.

bound fashion. Interestingly, C2C12 exhibited very different responses to homogeneous films presenting matrix-bound BMP-2 and BMP-7 (Fig. 2B). Whereas response to BMP-2 was steep (on/off mechanism), C2C12 responded more linearly to BMP-7.

In addition, we combined LbL assembly with a simple microfluidic channel to generate matrix-bound growth factor gradients. This method does not require a chemical modification of the growth factor or expensive equipment. The BMP gradients were maintained throughout the multiple days of cell culture whilst being bioactive. Importantly, the BMP adsorbed amounts can be tuned depending on the initial concentration of the BMP drops. In our experimental conditions, the maximum adsorbed amounts were 2 and 2.5 μg/cm^2 for BMP-2 and BMP-7 respectively and the gradient slope were 0.58 μg/cm^3 for BMP-2 and 1.24 μg/cm^3 for BMP-7.

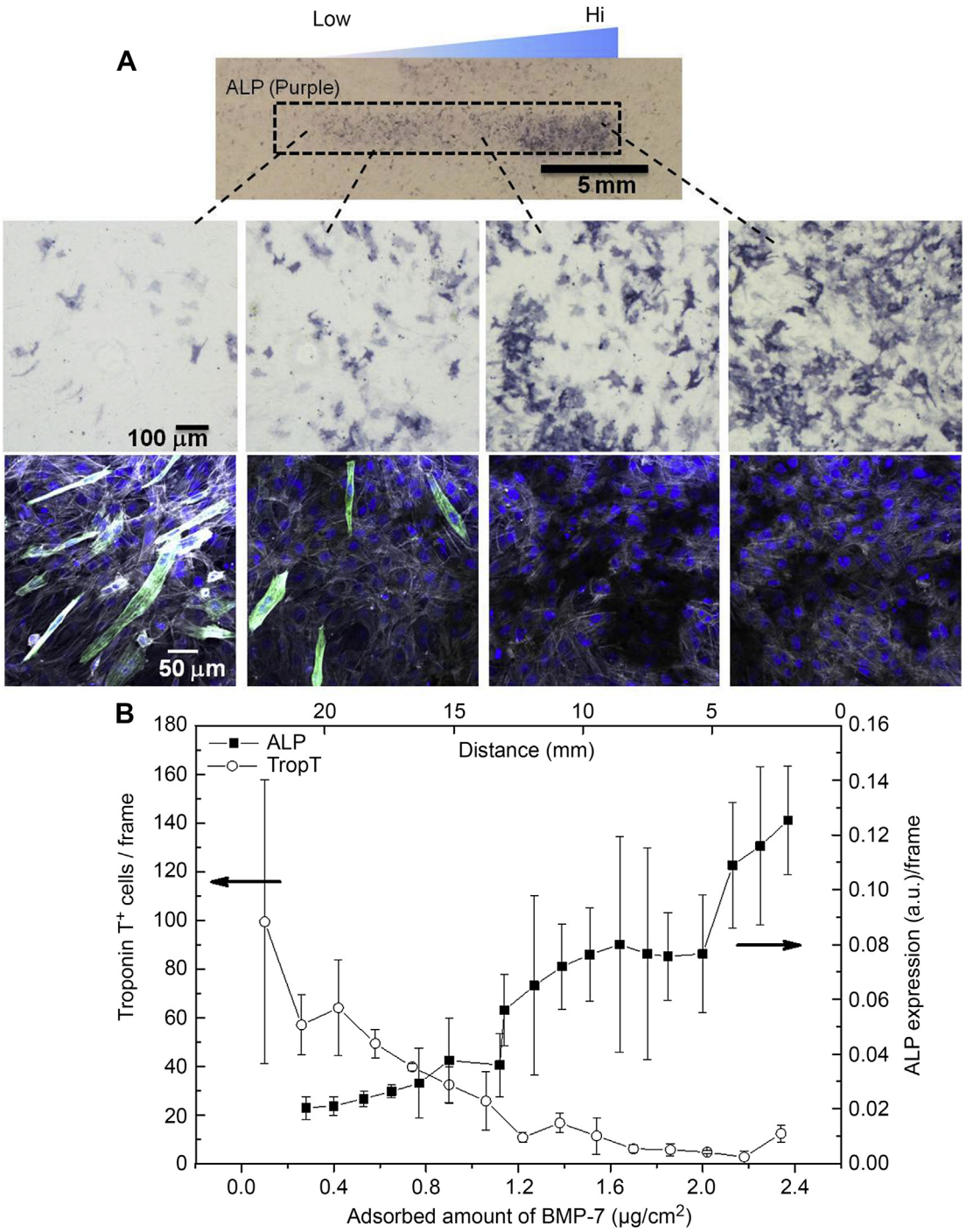

Fig. 6. Differentiation of C2C12 myoblasts on BMP-7 gradients. (A) Overview image and representative images of ALP staining confirms osteogenic differentiation, while immunofluorescent imaging reveals a decrease of troponin T positive cells with increasing BMP-7 concentration. Top images: ALP (purple); bottom images ALP (black), troponin T (green), actin (gray), nucleus (blue). (B) Quantification of ALP expression by measuring the intensities of the cyan and magenta channels in CMYK images, and amount of troponin T positive cells per field of view.

To our knowledge, only two other techniques have been proposed for generating BMP surface gradients either by chemical grafting or by natural affinity, which were applied solely to BMP-2. Samitier and coworkers [60] recently prepared a gradient of BMP-2 by grafting biotinylated BMP-2 to a gradient of carboxylate groups created on a PMMA surface via hydrolysis. This method yielded a maximum BMP-2 surface concentration of 0.04 μg/cm^2, which is at the lower end of our matrix-bound BMP-2 gradients. The BMP-2 gradients had also shallow slopes of 0.9 pmol/cm^3 (or 0.04 μg/cm^3) over a length of 80 mm. Interestingly, they also observed a non-linear expression of the osteogenic factors osterix and ALP in C2C12 cells but did not report myogenic commitment in the absence of BMP-2. While this approach for generating BMP-2 surface gradients is promising, it requires a hydrolyzable substrate and the biotinylation of the growth factor, which may affect its bioactivity. Besides, the amount of BMP-2 presented to the cells is low.

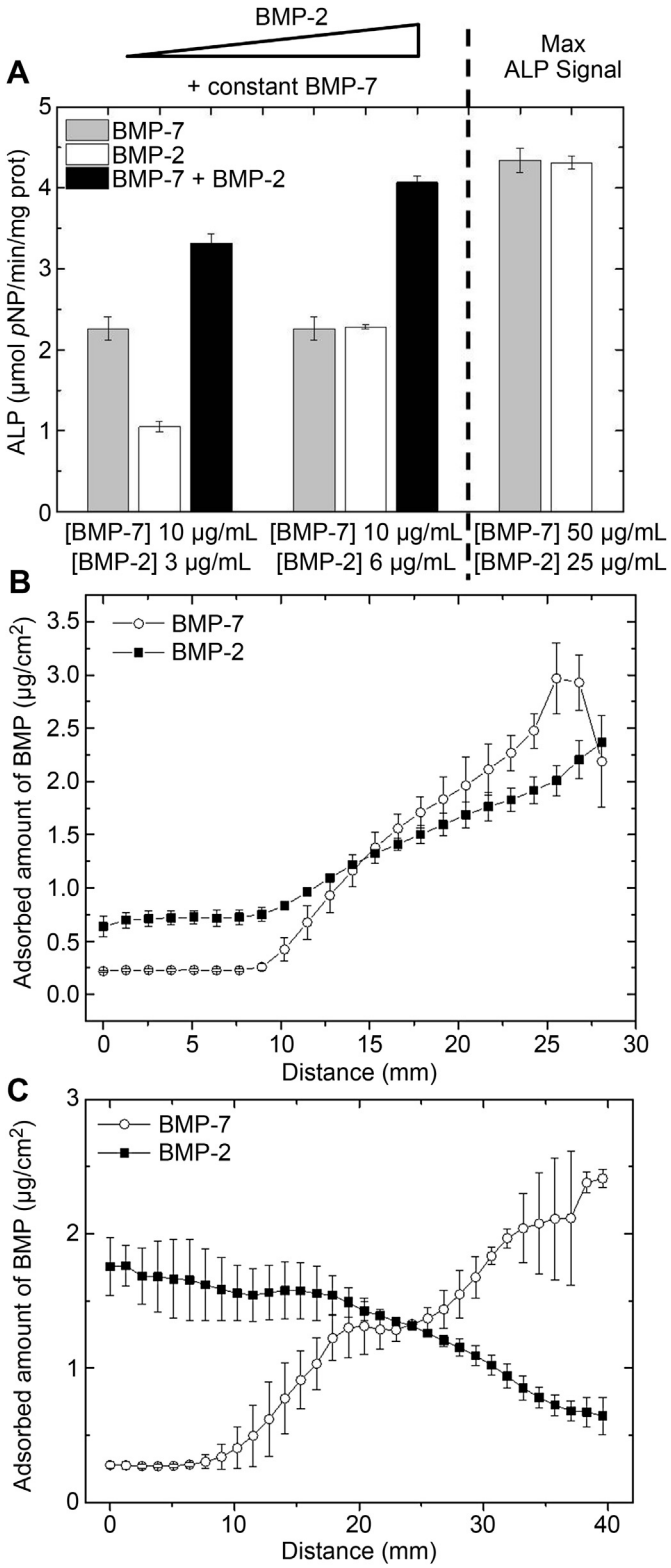

Fig. 7. (A) ALP expression of C2C12 myoblasts on (PLL/HA) films loaded with BMP-7 (gray bar), BMP-2 (white bars) or both (black bars). BMP-7 loading concentration was fixed to 10 μg/mL (corresponding to 0.38 μg/cm^2) and BMP-2 loading concentration to 3 or 6 μg/mL (corresponding to 0.19 and 0.38 μg/cm^2). On the right hand side is plotted ALP signal when BMP-7 is incorporated from a solution at 50 μg/mL (corresponding to 1.76 μg/cm^2) and BMP-2 from a solution at 25 μg/mL (corresponding to 1.16 μg/cm^2). Additive effect on ALP is observed when both BMPs are delivered from the same film. (B) Profiles of matrix-bound dual parallel BMP-2 and -7 gradients as a function of length of the channels. (C) Profiles of dual opposite BMP-2 and BMP-7 gradients. Adsorbed amounts were calculated as indicated in Fig. 3. Error bars indicate standard deviation between three different channels.

Another strategy was proposed by Campbell and coworkers, who used inkjet printing of BMP-2 on fibrin-coated substrates [32,10], each spot being close to 50 μm in diameter. Similarly to the (PLL/HA) films, fibrin enables myogenic differentiation in the absence of matrix-bound BMP-2. Doing overprints allowed them to increase the BMP-2 adsorbed amount up to 0.32 μg/cm^2 [61]. In addition, by moving laterally the nozzle with lateral steps ~70–200 μm, they created almost linear gradients [61] with a slope of 0.248 μg/cm^3 over 1.5 mm. This inkjet printing approach is attractive as it can be used in any type of substrate [11] and can generate gradients of different profiles (i.e. linear vs. exponential). However, the limitation relies in the size/spatial resolution of the deposited liquid droplet and in the complexity of the custom made inkjet deposition system.

Here, the behavior of C2C12 myoblasts differed on the different matrix-bound BMPs gradients generated on the biomimetic films. A non-linear ALP expression was observed on BMP-2 gradients with an on/off response, where ALP expression increased in a step fashion in a short window of the gradient whilst myogenic markers decreased in a similar way (Fig. 5B). In contrast, there was a linear dose response of myoblasts seeded on the matrix-bound BMP-7 gradient with regards to both ALP and troponin T expression (Fig. 6B). Both the ALP data on homogenous films and on gradients confirmed that BMP-2 is more potent than BMP-7 at stimulating ALP expression and suppressing myogenic markers (Figs. 1, 2, 5 and 6). Our data with matrix-bound BMP-2 and 7 gradients are thus in line with previous studies comparing ALP expression of C2C12 in the presence of soluble BMP-2 or BMP-7 [35,62,55].

We observed complete saturation of ALP expression on the parallel matrix-bound BMPs gradients (ALP value of 0.10–0.20), even at the end of the gradients where the BMP concentration was the lowest (Fig. 8), suggesting an additive or synergistic effect. This plateau was close to that observed for BMP-2 (Fig. 5B) and BMP-7 (Fig. 6B) individually. This effect was further confirmed by loading (PLL/HA) films with both BMP-2 and -7 homogenously (Fig. 7A). Previous reports observed a similar synergistic effect when delivering combinations of different BMPs in solution on MG-63 osteoblast-like cells [63] and C2C12 myoblasts [62]. In particular, whereas individual infection of C2C12 cells by adenovirus for BMP-10, BMP-12, or BMP-13 did not induce osteogenic differentiation, some of the co-infected cells (BMP-7 + BMP-10, BMP-7 + BMP-12 + BMP-7 + BMP-13) were able to drive osteogenic differentiation. This suggests a synergistic effect between two different BMPs. Interestingly, biomaterials for the simultaneous or sequential delivery of BMP-2 and BMP-7 have been developed by Hasirci et al. [64]. In all instances they observe that a sequential delivery yields higher ALP expression of bone-marrow mesenchymal stem cells.

The versatility and simplicity of both LbL films and microfluidic techniques opens interesting perspectives. The LbL strategy allows for the selection of any polyelectrolyte pair, thus easily modifying the surface chemistry and opening numerous possibilities for the deposit of various growth factors. For instance, other polyeletrolyte films are known to efficiently adsorb FGF-2 [24,13], BDNF [22] or VEGF [23] and, more importantly, to preserve their bioactivity. The microfluidic system used here is simple and can already generate dual BMP gradients either parallel (Fig. 7B) or opposite (Fig. 7C). Thus, it may be easily applied to generate matrix-bound gradients of other types of growth factors on films of different chemistries. In addition, it may be envisioned to develop more complex microfluidic devices in order to perform gradients of different profiles. These matrix-bound growth factor gradients may also be used to test in a high-throughput manner drug effects on cellular responses.

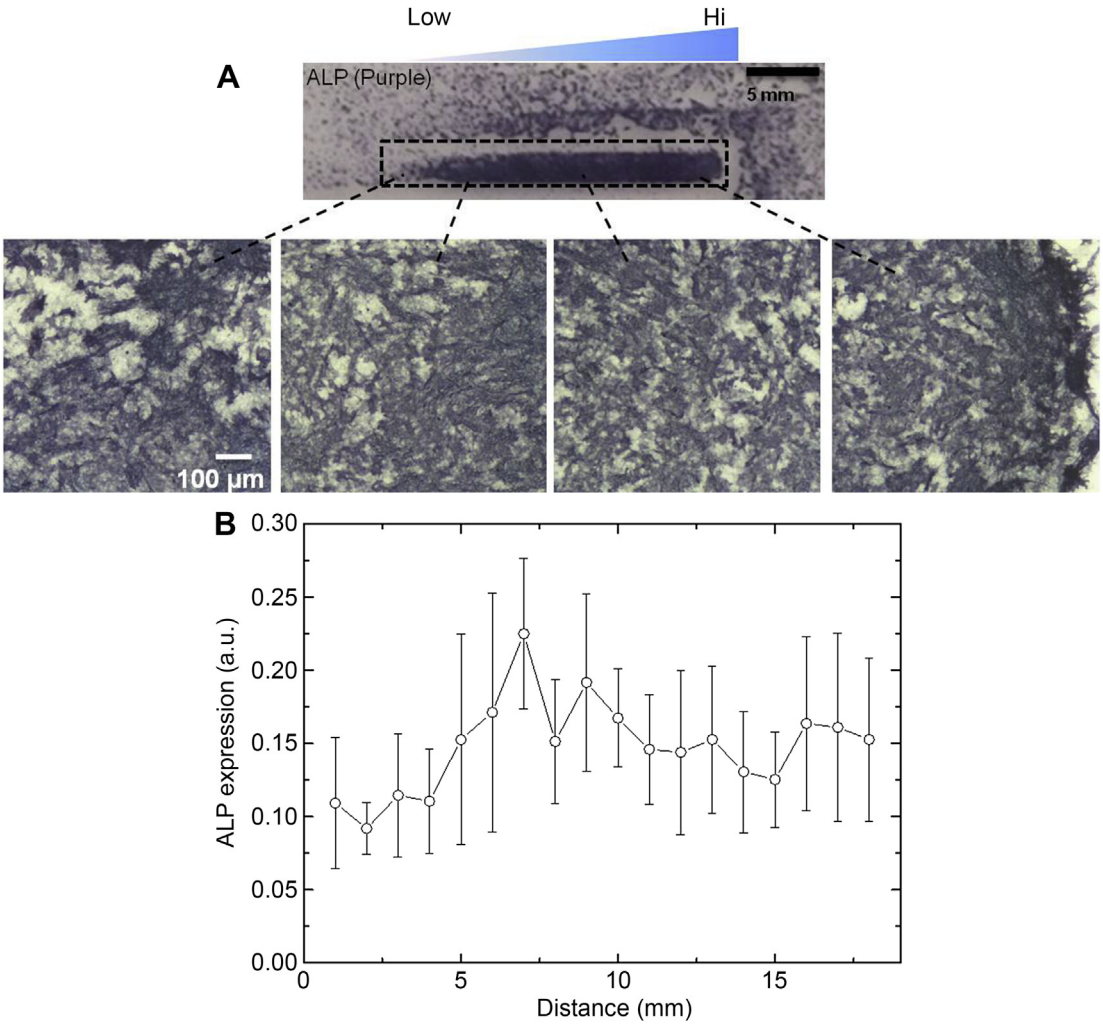

Fig. 8. Differentiation of C2C12 myoblasts on dual parallel BMP-2 and -7 gradients. (A) Overview image and representative images of ALP staining confirms osteogenic differentiation. no troponin T positive cells were found. (B) Quantification of ALP expression by measuring the intensities of the cyan and magenta channels in CMYK images.

5. Conclusions

In this work, we have presented a flexible platform for the generation of matrix-bound growth factor gradients by combining the LbL technique with microfluidics. Gradients of both BMP-2 and BMP-7 were generated and tested for their bioactivity. We observed that the osteogenic response of myoblasts to the matrix-bound BMP gradients varies with the selection of the growth factor. Moreover, this technology allows for the generation of dual gradients of growth factors in either parallel or opposite direction. Investigations of the potential synergistic or competitive effects that different combinations of growth factors might have on various cellular process in an ECM mimetic material is thus possible. The versatility of the LbL technique makes it adaptable for other polyelectrolyte pairs, easily tuning the chemistry of the system and other growth factors. Also, this combined microfluidic/LbL platform has the potential to simultaneously investigate various cellular signals (mechanical vs. biochemical) on the same substrate.

Acknowledgments

This work was supported by the European Commission (under FP7) via an ERC starting grant (BIOMIM, GA 259370) to CP and by the Whitaker International Program by providing JA with a postdoctoral scholarship. The authors thank Thibaut Galtier and Imran MacMillan for their assistance on BMP gradient characterization, T. Crouzier for fruitful discussions and H. Kim for careful reading of the manuscript. The authors thank D. Logeart-Avramoglou for providing the C2C12-A5 cells and Olympus Biotech for providing recombinant human BMP-7. The authors declare no financial interest.

Appendix A. Supplementary material

Supplementary material related to this article can be found at http://dx.doi.org/10.1016/j.biomaterials.2014.01.012.

References

[1] Hynes RO. The extracellular matrix: not just pretty fibrils. Science 2009;326:1216–9.
[2] Keung AJ, Kumar S, Schaffer DV. Presentation counts: microenvironmental regulation of stem Cells by biophysical and material cues. In: Schekman R, Goldstein L, Lehmann R, editors. Annu Rev Cell Dev Biol, 26; 2010. pp. 533–56. Annual Reviews, Palo Alto.
[3] Lortat-Jacob H. The molecular basis and functional implications of chemokine interactions with heparan sulphate. Curr Opin Struct Biol 2009;19:543–8.
[4] Martino MM, Hubbell JA. The 12th–14th type III repeats of fibronectin function as a highly promiscuous growth factor-binding domain. FASEB J 2010;24:4711–21.
[5] Brizzi MF, Tarone G, Defilippi P. Extracellular matrix, integrins, and growth factors as tailors of the stem cell niche. Curr Opin Cell Biol 2012;24:645–51.
[6] Dong X, Wang Q, Wu T, Pan H. Understanding adsorption–desorption dynamics of BMP-2 on hydroxyapatite (001) surface. Biophys J 2007;93:750–9.

[7] Lee K, Silva EA, Mooney DJ. Growth factor delivery-based tissue engineering: general approaches and a review of recent developments. J R Soc Interface 2011;8:153–70.
[8] Hudalla GA, Murphy WL. Biomaterials that regulate growth factor activity via bioinspired interactions. Adv Funct Mater 2011;21:1754–68.
[9] Masters KS. Covalent growth factor immobilization strategies for tissue repair and regeneration. Macromol Biosci 2011;11:1149–63.
[10] Ker EDF, Chu B, Phillippi JA, Gharaibeh B, Huard J, Weiss LE, et al. Engineering spatial control of multiple differentiation fates within a stem cell population. Biomaterials 2011;32:3413–22.
[11] Ker EDP, Nain AS, Weiss LE, Wang J, Suhan J, Amon CH, et al. Bioprinting of growth factors onto aligned sub-micron fibrous scaffolds for simultaneous control of cell differentiation and alignment. Biomaterials 2011;32:8097–107.
[12] Casper CL, Yang WD, Farach-Carson MC, Rabolt JF. Coating electrospun collagen and gelatin fibers with perlecan domain I for increased growth factor binding. Biomacromolecules 2007;8:1116–23.
[13] Almodovar J, Bacon S, Gogolski J, Kisiday JD, Kipper MJ. Polysaccharide-based polyelectrolyte multilayer surface coatings can enhance mesenchymal stem cell response to adsorbed growth factors. Biomacromolecules 2010;11:2629–39.
[14] Crouzier T, Ren K, Nicolas C, Roy C, Picart C. Layer-by-layer films as a biomimetic reservoir for rhBMP-2 delivery: controlled differentiation of myoblasts to osteoblasts. Small 2009;5:598–608.
[15] Campbell PG, Miller ED, Fisher GW, Walker LM, Weiss LE. Engineered spatial patterns of FGF-2 immobilized on fibrin direct cell organization. Biomaterials 2005;26:6762–70.
[16] Liu L, Ratner BD, Sage EH, Jiang S. Endothelial cell migration on surface-density gradients of fibronectin, VEGF, or both proteins. Langmuir 2007;23:11168–73.
[17] Martino MM, Tortelli F, Mochizuki M, Traub S, Ben-David D, Kuhn GA, et al. Engineering the growth factor microenvironment with fibronectin domains to promote wound and bone tissue healing. Sci Transl Med 2011;3. 100ra89.
[18] Decher G. Fuzzy nanoassemblies: toward layered polymeric multicomposites. Science 1997;277:1232–7.
[19] Boudou T, Crouzier T, Ren K, Blin G, Picart C. Multiple functionalities of polyelectrolyte multilayer films: new biomedical applications. Adv Mater 2010;22:441–67.
[20] Detzel CJ, Larkin AL, Rajagopalan P. Polyelectrolyte multilayers in tissue engineering. Tissue Eng Part B Rev 2011;17:101–13.
[21] Shah NJ, Hong J, Hyder MN, Hammond PT. Osteophilic multilayer coatings for accelerated bone tissue growth. Adv Mater 2012;24:1445–50.
[22] Vodouhe C, Schmittbuhl M, Boulmedais F, Bagnard D, Vautier D, Schaaf P, et al. Effect of functionalization of multilayered polyelectrolyte films on motoneuron growth. Biomaterials 2005;26:545–54.
[23] Muller S, Koenig G, Charpiot A, Debry C, Voegel J, Lavalle P, et al. VEGF-functionalized polyelectrolyte multilayers as proangiogenic prosthetic coatings. Adv Funct Mater 2008;18:1767–75.
[24] Ma L, Zhou J, Gao C, Shen J. Incorporation of basic fibroblast growth factor by a layer-by-layer assembly technique to produce bioactive substrates. J Biomed Mater Res B Appl Biomater 2007;83B:285–92.
[25] Crouzier T, Fourel L, Boudou T, Albiges-Rizo C, Picart C. Presentation of BMP-2 from a soft biopolymeric film unveils its activity on cell adhesion and migration. Adv Mater 2011;23:H111–8.
[26] Rogers KW, Schier AF. Morphogen gradients: from generation to interpretation. In: Schekman R, Goldstein L, Lehmann R, editors. Annu Rev Cell Dev Biol, 27; 2011. pp. 377–407. Annual Reviews, Palo Alto.
[27] Edalat F, Sheu I, Manoucheri S, Khademhosseini A. Material strategies for creating artificial cell-instructive niches. Curr Opin Biotechnol 2012;23:820–5.
[28] Lai N, Sims JK, Jeon NL, Lee K. Adipocyte induction of preadipocyte differentiation in a gradient chamber. Tissue Eng Part C-Methods 2012;18:958–67.
[29] Wong KHK, Chan JM, Kamm RD, Tien J. Microfluidic models of vascular functions. In: Yarmush ML, editor. Annu Rev Biomed Eng, 14; 2012. pp. 205–30. Annual Reviews, Palo Alto.
[30] Kim BJ, Hannanta-Anan P, Chau M, Kim YS, Swartz MA, Wu MM. Cooperative roles of SDF-1 alpha and EGF Gradients on tumor cell migration revealed by a robust 3D microfluidic model. PLoS One 2013;8.
[31] Stefonek-Puccinelli TJ, Masters KS. Co-immobilization of gradient-patterned growth factors for directed cell migration. Annu Rev Biomed Eng 2008;36:2121–33.
[32] Phillippi JA, Miller E, Weiss L, Huard J, Waggoner A, Campbell P. Microenvironments engineered by inkjet bioprinting spatially direct adult stem cells toward muscle- and bone-like subpopulations. Stem Cells 2008;26:127–34.
[33] Miller ED, Li K, Kanade T, Weiss LE, Walker LM, Campbell PG. Spatially directed guidance of stem cell population migration by immobilized patterns of growth factors. Biomaterials 2011;32:2775–85.
[34] Obradovic Wagner D, Sieber C, Bhushan R, Borgermann JH, Graf D, Knaus P. BMPs: from bone to body morphogenetic proteins. Sci Signal 2010;3. mr1.
[35] Cheng H, Jiang W, Phillips FM, Haydon RC, Peng Y, Zhou L, et al. Osteogenic activity of the fourteen types of human bone morphogenetic proteins (BMPs). J Bone Joint Surg Am 2003;85:1544–52.
[36] Axelrad TW, Einhorn TA. Bone morphogenetic proteins in orthopaedic surgery. Cytokine Growth F R 2009;20:481–8.
[37] Kim HD, Valentini RF. Retention and activity of BMP-2 in hyaluronic acid-based scaffolds in vitro. J Biomed Mater Res 2002;59:573–84.
[38] Haidar ZS, Hamdy RC, Tabrizian M. Delivery of recombinant bone morphogenetic proteins for bone regeneration and repair. Part B: delivery systems for BMPs in orthopaedic and craniofacial tissue engineering. Biotechnol Lett 2009;31:1825–35.
[39] Boerckel JD, Kolambkar YM, Dupont KM, Uhrig BA, Phelps EA, Stevens HY, et al. Effects of protein dose and delivery system on BMP-mediated bone regeneration. Biomaterials 2011;32:5241–51.
[40] Smith DM, Cray JJJ, Weiss LE, Dai Fei EK, Shakir S, Rottgers SA, et al. Precise control of osteogenesis for craniofacial defect repair: the role of direct osteoprogenitor contact in BMP-2-based bioprinting. Ann Plast Surg 2012;69:485–8. 10.1097/SAP.0b013e31824cfe64.
[41] Murali S, Rai B, Dombrowski C, Lee JLJ, Lim ZXH, Bramono DS, et al. Affinity-selected heparan sulfate for bone repair. Biomaterials 2013;34:5594–605.
[42] Ramel MC, Hill CS. Spatial regulation of BMP activity. FEBS Lett 2012;586:1929–41.
[43] Ramel MC, Hill CS. The ventral to dorsal BMP activity gradient in the early zebrafish embryo is determined by graded expression of BMP ligands. Dev Biol 2013;378:170–82.
[44] Buket Basmanav F, Kose GT, Hasirci V. Sequential growth factor delivery from complexed microspheres for bone tissue engineering. Biomaterials 2008;29:4195–204.
[45] Yilgor P, Tuzlakoglu K, Reis RL, Hasirci N, Hasirci V. Incorporation of a sequential BMP-2/BMP-7 delivery system into chitosan-based scaffolds for bone tissue engineering. Biomaterials 2009;30.
[46] Du Y, Shim J, Vidula M, Hancock MJ, Lo E, Chung BG, et al. Rapid generation of spatially and temporally controllable long-range concentration gradients in a microfluidic device. Lab Chip 2009;9:761–7.
[47] Almodovar J, Crouzier T, Selimovic S, Boudou T, Khademhosseini A, Picart C. Gradients of physical and biochemical cues on polyelectrolyte multilayer films generated via microfluidics. Lab Chip 2013;13:1562–70.
[48] Katagiri T, Akiyama S, Namiki M, Komaki M, Yamaguchi A, Rosen V, et al. Bone morphogenetic protein-2 inhibits terminal differentiation of myogenic cells by suppressing the transcriptional activity of MyoD and myogenin. Exp Cell Res 1997;230:342–51.
[49] Yeh LCC, Tsai AD, Lee JC. Osteogenic protein-1 (OP-1, BMP-7) induces osteoblastic cell differentiation of the pluripotent mesenchymal cell line C2C12. J Cell Biochem 2002;87:292–304.
[50] Schneider A, Francius G, Obeid R, Schwinte P, Hemmerle J, Frisch B, et al. Polyelectrolyte multilayers with a tunable Young's modulus: influence of film stiffness on cell adhesion. Langmuir 2006;22:1193–200.
[51] Logeart-Avramoglou D, Bourguignon M, Oudina K, Ten Dijke P, Petite H. An assay for the determination of biologically active bone morphogenetic proteins using cells transfected with an inhibitor of differentiation promoter-luciferase construct. Anal Biochem 2006;349:78–86.
[52] Gilde F, Maniti O, Guillot R, Mano JF, Logeart-Avramoglou D, Sailhan F, et al. Secondary structure of rhBMP-2 in a protective biopolymeric carrier material. Biomacromolecules 2012;13:3620–6.
[53] Crouzier T, Sailhan F, Becquart P, Guillot R, Logeart-Avramoglou D, Picart C. The performance of BMP-2 loaded TCP/HAP porous ceramics with a polyelectrolyte multilayer film coating. Biomaterials 2011;32:7543–54.
[54] Guillot R, Gilde F, Becquart P, Sailhan F, Lapeyrere A, Logeart-Avramoglou D, et al. The stability of BMP loaded polyelectrolyte multilayer coatings on titanium. Biomaterials 2013;34:5737–46.
[55] Barr T, McNamara AJA, Sándor GKB, Clokie CML, Peel SAF. Comparison of the osteoinductivity of bioimplants containing recombinant human bone morphogenetic proteins 2 (Infuse) and 7 (OP-1). Oral Surg. Oral Med. Oral Pathol. Oral Radiol 2010;109:531–40.
[56] van den Beucken JJJP, Walboomers XF, Boerman OC, Vos MRJ, Sommerdijk NAJM, Hayakawa T, et al. Functionalization of multilayered DNA-coatings with bone morphogenetic protein 2. J Control Release 2006;113:63–72.
[57] Crouzier T, Szarpak A, Boudou T, Auzely-Velty R, Picart C. Polysaccharide-blend multilayers containing hyaluronan and heparin as a delivery system for rhBMP-2. Small 2010;6:651–62.
[58] Haidar ZS, Azari F, Hamdy RC, Tabrizian M. Modulated release of OP-1 and enhanced preosteoblast differentiation using a core-shell nanoparticulate system. J Biomed Mater Res A 2009;91A:919–28.
[59] Haidar ZS, Hamdy RC, Tabrizian M. Biocompatibility and safety of a hybrid core–shell nanoparticulate OP-1 delivery system intramuscularly administered in rats. Biomaterials 2010;31:2746–54.
[60] Lagunas A, Comelles J, Oberhansl S, Hortigüela V, Martínez E, Samitier J. Continuous bone morphogenetic protein-2 gradients for concentration effect studies on C2C12 osteogenic fate. Nanomed Nanotechnol Biol Med 2013;9:694–701.
[61] Miller ED, Phillippi JA, Fisher GW, Campbell PG, Walker LM, Weiss LE. Inkjet printing of growth factor concentration gradients and combinatorial arrays immobilized on biologically-relevant substrates. Comb Chem High Throughput Screen 2009;12:604–18.
[62] Luu HH, Song W-X, Luo X, Manning D, Luo J, Deng Z-L, et al. Distinct roles of bone morphogenetic proteins in osteogenic differentiation of mesenchymal stem cells. J Orthop Res 2007;25:665–77.
[63] Laflamme C, Rouabhia M. Effect of BMP-2 and BMP-7 homodimers and a mixture of BMP-2/BMP-7 homodimers on osteoblast adhesion and growth following culture on a collagen scaffold. Biomed Mater 2008;3:015008.
[64] Yilgor P, Hasirci N, Hasirci V. Sequential BMP-2/BMP-7 delivery from polyester nanocapsules. J Biomed Mater Res A 2010;93A:528–36.